DFT and DFT-D3 Studies of Glycerol Adsorption on the Cu(111), Cu(100), and Cu(110) Surfaces

Frannie Drake, Peshala K. Jayamaha, and Lichang Wang*

School of Chemical and Biomolecular Sciences, Southern Illinois University Carbondale, Carbondale, IL 62901, USA

Abstract

Adsorption of glycerol is the first step in many catalytic reactions to transform glycerol that was formed as biodiesel byproduct into valuable products. Among many feasible catalysts, Cu seems to be a good choice due to its abundance and cost consideration, though extensive studies are needed to evaluate the performance of Cu catalysts on glycerol transformation. Density functional theory (DFT) calculations and van der Waals corrected calculations (DFT-D3) were therefore performed in this work to study the adsorption of glycerol on the three most abundant copper surfaces: Cu(111), Cu(100), and Cu(110). Inclusion of the van der Waals interactions resulted in higher adsorption energies and shorter Cu-O bond distances. The most favorable adsorption location was determined to be the Cu(110) long bridge site. The strongest adsorption is the atop site on the Cu(111) and the hollow site on the Cu(100), though the other adsorption sites are also very favorable.

* Corresponding author: lwang@chem.siu.edu

1. Introduction

Biodiesel is widely recognized as a renewable alternative to fossil diesel, and its production has increased significantly since 2010. Soybean oil is a major feedstock to biodiesel production, and the manufacturing associated with biodiesel will undoubtedly affect the soybean industry.[1] Glycerol is an unavoidable and massive byproduct from biodiesel manufacturing; about 10 kg of crude glycerol is produced for every 100 kg of biodiesel generated. The increase in biodiesel production has resulted in an excess of glycerol and lead to the lower price of glycerol, which has a negative impact in the biodiesel industry by causing an increase in the operating cost to ~$0.15 per gal of biodiesel.[1] One opportunity to reduce the cost of biodiesel production, and therefore promote Illinois soybean production, is to use it as fuel in fuel cells[2-17] or search for ways of transforming glycerol into fuels and chemicals[1] coupled with CO_2 utilization[18] and other value added species.[19-22] The urgent need for studies of glycerol transformation to the value-added chemicals for use in many industry fields such as in solar cells[23-37] has inspired many studies and makes research on catalytic glycerol transformation an important, active area.[18,38-101]

Purified glycerol can be used in direct glycerol fuel cells, which is comparable in energy density to ethanol fuel cells. More importantly, glycerol can be turned into many value-added products ranging from pharmaceutical and agricultural precursors to fine chemicals. However, the progress in glycerol transformation to value-added chemicals is hindered by the selectivity and poor energy efficiency of the molecule. For example, in the study of catalytic oxidehydration of glycerol, a variety of products were formed: glycidol, hydroxyacetone, methylglyoxal, glycerol formal, formaldehyde, formic acid, ethanol, acetaldehyde, acetic acid, 1,3-propane dioldiacetate, acrylic acid, acrolein, and oxalic acid, to name a few.[102] The abundance of products generated is due to the selectivity of each elementary step involved in the reaction; consider, glycerol has four

different hydrogen atoms that could be removed during a deprotonation. Additionally, energy efficiency is an important concern during glycerol transformation. Au has been studied as an efficient catalyst for glycerol transformations,[103] and a computational study conducted with glycerol on Au with transition metal alloys proposed that Pt, Pd, Sn, and Cu could be potential alloys to efficiently deprotonate glycerol.[104] The most studied heterogeneous catalysts include Pt,[105] Pd,[106-108] and Ir[109-115] for various reactions. In comparison to these metals, Cu is abundant and relatively inexpensive, making it an ideal candidate for a cost-effective catalyst. In the conversion of ethanol to ethyl acetate, Cu as catalyst was used experimentally[116,117] and studied in density functional theory (DFT) calculations.[118-120] Therefore, we used computational modeling to study the adsorption of glycerol on copper, the first step in evaluating it as a potential catalyst for glycerol chemistry.

The objectives of this work are to make comparative studies of glycerol adsorption on the Cu surfaces and to understand the effect of surface features on the adsorption process. Towards these, DFT calculations were performed to determine the adsorption energies of glycerol docked on the different sites of the three most abundant surfaces in copper nanoparticles: Cu(111), Cu(100), and Cu(110). Inclusion of van der Waals interactions in DFT calculations (DFT-D3) was found to increase the adsorption energy, lower the reaction barrier, and more accurately predict reaction pathways with weak adsorptions,[121] but did not change the order of favored surfaces, merely the factor of difference between their energies.[122,123] As such, we conducted both DFT and DFT-D3 calculations to determine and understand the differences in adsorption energies on account of van der Waals corrections.

2. Computational Details

The model surfaces of Cu catalysts were built directly from the bulk Cu crystals. The Cu-bulk crystal was optimized first and then cleaved to form the Cu(111), Cu(100), and Cu(110) surfaces. Three layer periodic slabs with (6x6), (5x5), and (4x10) supercell surfaces, respectively, were constructed with a 15 Å vacuum added in the z direction where glycerol molecule is to be adsorbed. Three layer slabs were used to reduce the number of atoms in the model to save memory and reduce computational time while maintaining the accuracy of the results, and also in conjunction with the three layer Cu slabs that were used in the DFT study of ethanol dimerization.[118] As such, the Cu(111) slab contained 108 Cu atoms, the Cu(100) slab contained 150 Cu atoms, and the Cu(110) slab contained 120 Cu atoms.

As seen in Figure 1, the Cu(111) surface has four different adsorption sites: bridge, atop, fcc, and hcp; the Cu(100) surface has three different adsorption sites: bridge, hollow, and atop; and the Cu(110) surface has four different adsorption sites: short bridge, long bridge, hollow, and atop. Once the Cu slabs were optimized, an optimized glycerol molecule was docked with its central oxygen atom oriented to each adsorption location with a bond length of approximately 2.4 Å between the oxygen and copper surface (see Fig. 2.). We note that a glycerol molecule can also take other adsorption configurations, such as those shown in the previous work[121,124,125] when adsorbed molecules are no longer to be methane, for low coverage, the parallel adsorption is most likely and we therefore take it as the initial configuration and allowed it to fully relax to other configurations. Future studies can be assisted by using molecular dynamics simulations to generate more adsorption configurations.[126,127]

In our calculations, the bottom layer of Cu atoms in the slab was fixed at their optimized positions, while the top two layers of Cu atoms and the adsorbate (glycerol) were allowed to relax.

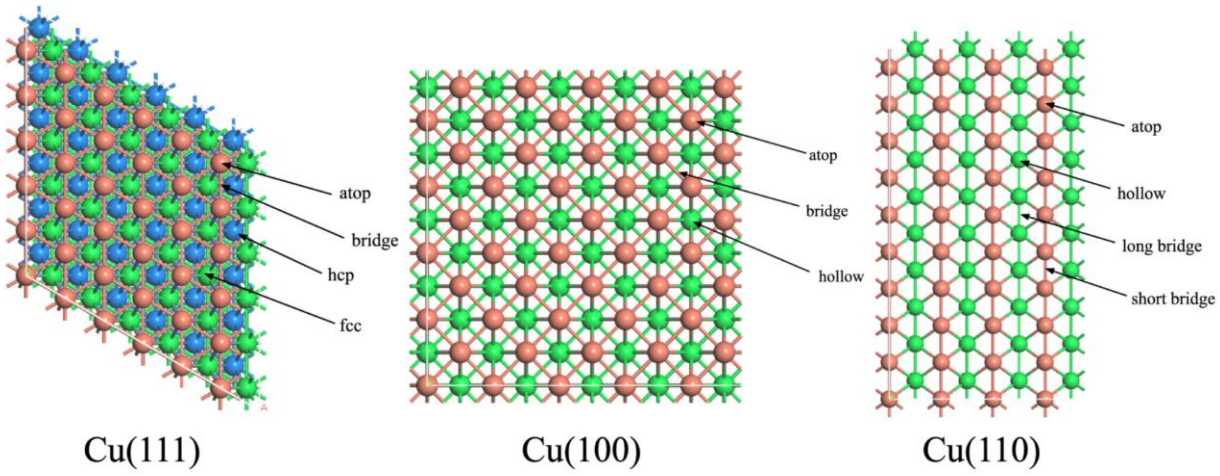

Fig. 1. Top view of Cu(111), Cu(100), and Cu(110) with labeled adsorption sites. Peach coloured balls represent the top layer of Cu, the green balls represent the second layer of Cu, and the blue balls represent the third (bottom) layer of Cu.

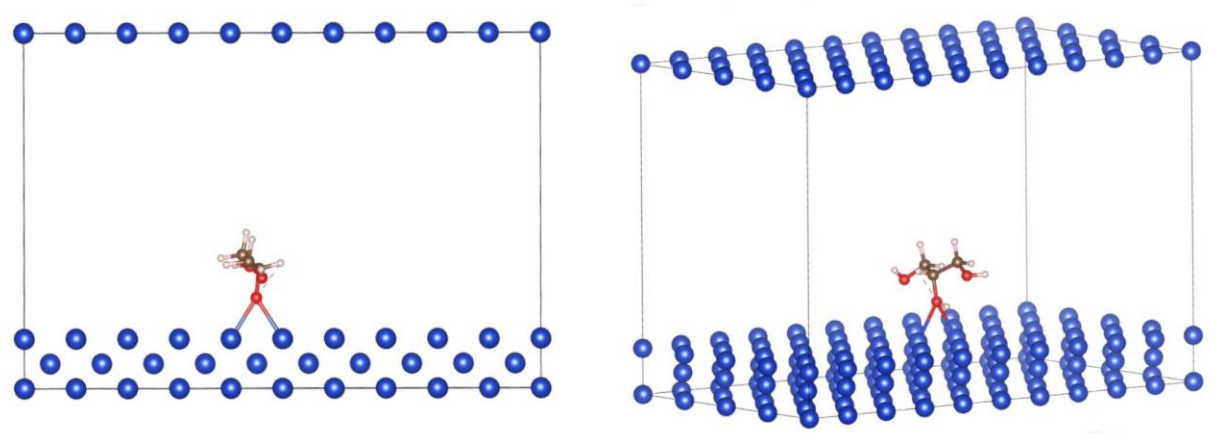

Fig. 2. View of glycerol adsorbed onto Cu(110) at the short bridge location.

All DFT calculations were performed using the Vienna ab initio simulation package (VASP).[128,129] The exchange-correlation energies were obtained using the Perdew-Burke-Ernzerhof (PBE) functional.[130] VASPKIT was used to generate the Monkhorst-Pack grid k-points and to perform analysis of the DFT results.[131] A plane-wave basis set was used for all calculations with a cutoff energy of 400 eV. A Fermi smearing of 0.2 eV was employed. The maximum force was set to be less than 0.03 eV/Å. The Becke-Johnson damping function was used in the DFT-

D3 method.[132,133] For the DFT-D3 calculations, CONTCAR output files of the DFT calculations were used as the POSCAR input files.

The adsorption, or binding, energy (E_{ads}) was calculated using:

$$E_{ads} = E_{(glycerol/surface)} - E_{(glycerol)} - E_{(surface)}, \quad (1)$$

in which $E_{(glycerol/surface)}$ is the total energy of the given Cu surface with glycerol, $E_{(glycerol)}$ is the energy of glycerol optimized in the gas phase, and $E_{(surface)}$ is the energy of the optimized given copper surface. No zero point energy corrections are included in the reported results.

3. Results

In this section, DFT and DFT-D3 results of glycerol adsorption on the Cu(111), Cu(100), and Cu(110) are presented in the first three subsections with the discussion followed in 3.4.

3.1 Adsorption on Cu(111)

The ground state energy (E0) of the Cu(111) slab was found to be -370.06 eV according to the DFT calculation and -411.331 eV according to the van der Waals corrected calculation (DFT-D3), which is proportional to its 108 Cu atoms. The ground state energy of the glycerol was calculated under the unit cell conditions as the Cu(111) slab; the E0 energy of glycerol was -76.23 eV for the DFT calculation and -76.49 eV for the DFT-D3 calculation.

Table 1 shows the adsorption energies of glycerol on the four docking sites of Cu(111) as well as various bond lengths of the adsorbed glycerol. The adsorption energies were calculated using Eq. (1) and the previously reported ground state energy (E0) DFT results for the copper slab and glycerol, and the calculation output energies for the entire system. Figure 3 shows the distance between the copper surface and the central oxygen of the adsorbed glycerol molecule.

Table 1
Adsorption energies and Glycerol bond lengths on Cu(111) from the DFT and DFT-D3 calculation results.

	DFT					
Site	Adsorption E (eV)	Cu-O Distance (Å)	O-H Distance (Å)	C_1-H Distance (Å)	C_2-H Distance (Å)	C_3-H Distance (Å)
atop	-0.29	2.287	0.985	1.109, 1.002	1.106	1.104, 1.034
bridge	-0.14	2.923, 2.928	0.984	1.105, 1.108	1.108	1.104, 1.105
hcp	-0.22	2.954	0.984	1.107, 1.101	1.107	1.105, 1.105
fcc	-0.25	2.591	0.984	1.105, 1.105	1.106	1.102, 1.108
	DFT-D3					
Site	Adsorption E (eV)	Cu-O Distance (Å)	O-H Distance (Å)	C_1-H Distance (Å)	C_2-H Distance (Å)	C_3-H Distance (Å)
atop	-1.12	2.177	0.991	1.115, 1.103	1.105	1.101, 1.060
bridge	-0.84	2.519, 2.619	0.992	1.108, 1.104	1.105	1.105, 1.105
hcp	-0.73	2.723	0.986	1.106, 1.101	1.106	1.105, 1.105
fcc	-1.11	2.220	0.988	1.103, 1.108	1.105	1.101, 1.118

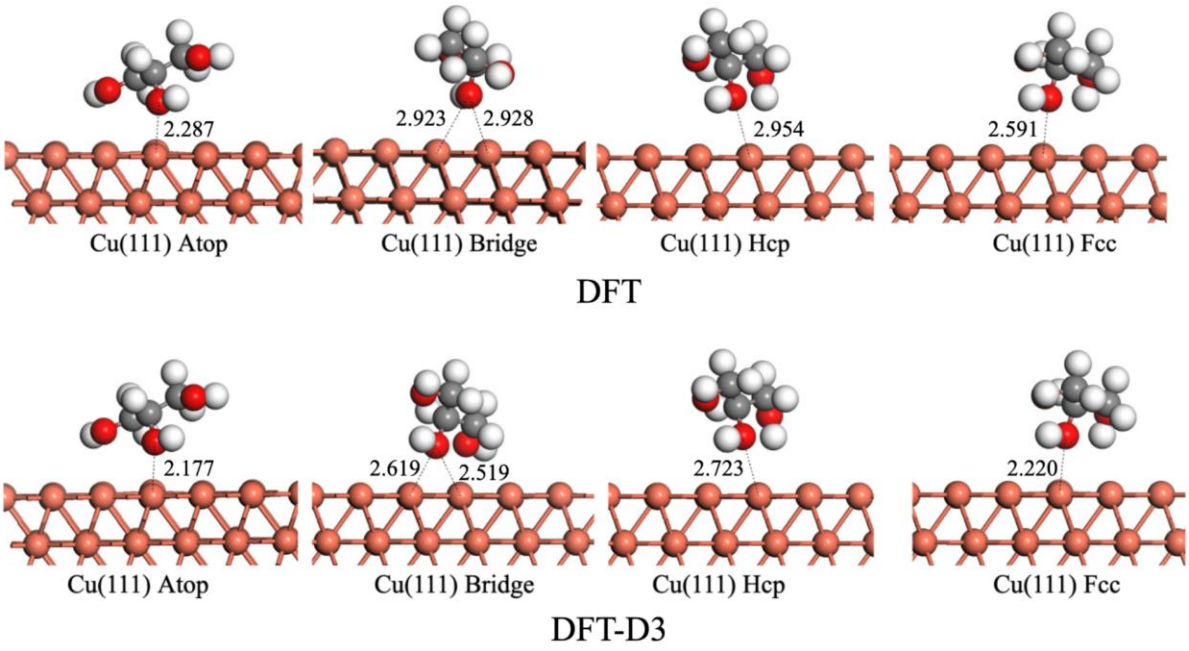

Fig. 3. Distance (Å) between the oxygen of the adsorbed glycerol and the copper surface for Cu(111) DFT (top) and DFT-D3 (bottom) calculation results.

For the Cu(111) surface, the atop site is the most stable according to both the DFT and DFT-D3 calculations because it has the highest adsorption energy. After the atop site, the fcc, and then the hcp sites are the next highest according to the DFT calculations, with the bridge site resulting in the lowest adsorption energy. While the DFT-D3 results agreed that the atop site is the most stable docking site on the Cu(111) surface, the bridge site surpassed the hcp site in adsorption energy, thus changing the order of site stability for this surface. We note that glycerol

adsorption energies on Cu(111) at different sites were also found to be -0.78~ -1.13 eV using PBE with D2 correction,[81] which agrees with the current studies.

As for the bond perturbation in the adsorbed glycerol molecule, the data shown in Table 1 indicates that small bond stretches can be seen and in general, the DTF-D3 bond distances, i.e. C-H and O-H bonds, in glycerol molecule are slightly longer than the DFT predicted. The Cu-O bonds from DFT-D3 calculations are considerably smaller than those from DFT calculations. Most of the adsorption configurations are the same between the DFT and DFT-D3 results, as shown in Figure 3. The only difference lies in the bridge site adsorption and this may explain on why the relative adsorption strength from DFT-D3 is different from that predicted from DFT.

3.2 Adsorption on Cu(100)

The Cu(100) slab contained 150 Cu atoms, and its ground state energy was found to be -498.41 eV according to the DFT calculation and -551.52 eV according to the DFT-D3 calculation. The ground state energy of the glycerol was calculated under the same unit cell conditions as the Cu(100) slab; the E0 energy of glycerol was -76.23 eV for the DFT calculation and -76.49 eV for the DFT-D3 calculation.

Table 2 shows the adsorption energies of glycerol on the three docking sites of Cu(100), as well as various bond lengths of the adsorbed glycerol. The adsorption energies were calculated in the same manner as the Cu(111) adsorptions. Figure 4 shows the distance between the copper surface and the central oxygen of the adsorbed glycerol molecule.

Table 2
Adsorption energies and Glycerol bond lengths on Cu(100) from the DFT and DFT-D3 calculation results.

	DFT					
Site	Adsorption E (eV)	Cu-O Distance (Å)	O-H Distance (Å)	C_1-H Distance (Å)	C_2-H Distance (Å)	C_3-H Distance (Å)
atop	-0.47	2.187	0.988	1.110, 1.051	1.105	1.103, 1.104
bridge	-0.41	2.348, 2.471	0.991	1.104, 1.104	1.104	1.104, 1.104
hollow	-0.38	2.339	0.985	1.101, 1.109	1.103	1.102, 1.106
	DFT-D3					
Site	Adsorption E (eV)	Cu-O Distance (Å)	O-H Distance (Å)	C_1-H Distance (Å)	C_2-H Distance (Å)	C_3-H Distance (Å)
atop	-1.03	2.138	0.990	1.102, 1.110	1.104	1.104, 1.103
bridge	-1.06	2.246, 2.400	0.993	1.103, 1.104	1.104	1.103, 1.104
hollow	-1.13	2.263	0.989	1.101, 1112	1.102	1.101, 1.107

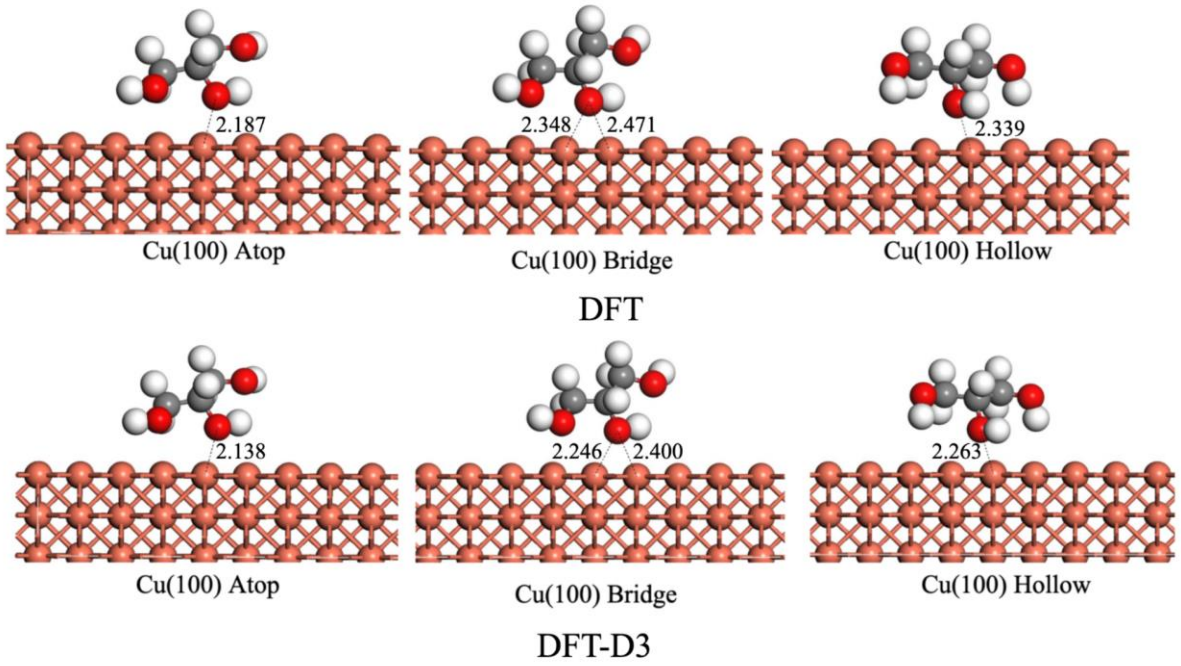

Fig. 4. Distance (Å) between the oxygen of the adsorbed glycerol and the copper surface for Cu(100) DFT (top) and DFT-D3 (bottom) calculation results.

The Cu(100) results for the DFT and DFT-D3 calculations were inverse. According to the DFT calculations, the Cu(100) atop is the most stable docking site and the Cu(100) hollow is the least stable docking site; however, according to the DFT-D3 calculations, the Cu(100) hollow is the most stable docking site and the Cu(100) atop is the least stable docking site. We note that

this is slightly different from the glycerol adsorption on Pt_6/Pt(100),[134] where DFT-D3 and DFT predicted the same strong adsorption site.

Various C-H and OH bonds of glycerol are slightly stretched upon adsorption as shown in Table 2 and the Cu-O distances vary between 2.1 – 2.5 Å. It is interesting to point out that for one of the end C atom, one C-H bond distance is shortened while the other lengthened from the DFT to DFT-D3 results. The adsorption configurations are remained very similar between DFT and DFT-D3 results as shown in Figure 4.

3.3 Adsorption on Cu(110)

The Cu(110) slab contained 120 Cu atoms. Its ground state energy was found to be -376.15 eV according to the DFT calculation and -409.08 eV according to the DFT-D3 calculation. The ground state energy of the glycerol was calculated under the same unit cell conditions as the Cu(110) slab; the E0 energy of glycerol was -76.23 eV for the DFT calculation and -76.49 eV for the DFT-D3 calculation.

Table 3 shows the adsorption energies of glycerol on the four docking sites of Cu(110), as well as various bond lengths of the adsorbed glycerol. The adsorption energies were calculated in the same manner as the Cu(111) adsorptions. Figure 5 shows the distance between the copper surface and the central oxygen of the adsorbed glycerol molecule.

Table 3
Adsorption energies and Glycerol bond lengths on Cu(110) from the DFT and DFT-D3 calculation results.

	DFT					
Site	Adsorption E (eV)	Cu-O Distance (Å)	O-H Distance (Å)	C_1-H Distance (Å)	C_2-H Distance (Å)	C_3-H Distance (Å)
atop	-0.52	2.177	0.986	1.103, 1.104	1.106	1.105, 1.104
hollow	-0.39	2.151	0.990	1.105,1.103	1.106	1.108, 1.107
long bridge	-0.53	2.175, 3.452	0.988	1.105, 1.103	1.102	1.107, 1.101
short bridge	-0.40	2.268, 2.431	0.990	1.108, 1.106	1.104	1.104, 1.105
	DFT-D3					
Site	Adsorption E (eV)	Cu-O Distance (Å)	O-H Distance (Å)	C_1-H Distance (Å)	C_2-H Distance (Å)	C_3-H Distance (Å)
atop	-1.06	2.118	0.987	1.103, 1.104	1.106	1.105, 1.104
hollow	-1.24	2.072	0.990	1.102, 1.112	1.104	1.111, 1.103
long bridge	-1.28	2.108, 3.255	0.991	1.100, 1.108	1.102	1.103, 1.107
short bridge	-1.21	2.196, 2.281	0.995	1.101, 1.111	1.103	1.103, 1.104

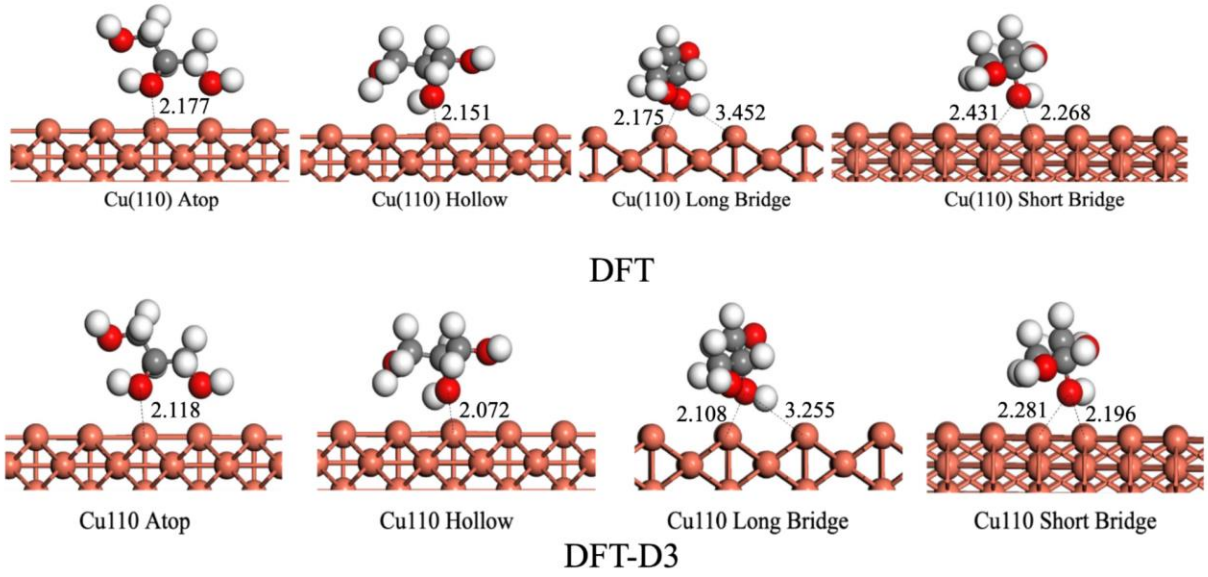

Fig. 5. Distance (Å) between the oxygen of the adsorbed glycerol and the copper surface for Cu(110) DFT (top) and DFT-D3 (bottom) calculation results.

According to the DFT calculations, Cu(110) long bridge and atop sites is the most ideal for docking glycerol due to the high adsorption energies required to remove the glycerol. The DFT-D3 calculation results suggest that Cu(110) long bridge, hollow, and short bridge is best for docking glycerol. The Cu(110) atop site was most likely not as stable according to the DFT-D3

calculations because the glycerol molecule was oriented above one particular atom, instead of over a bridge or hollow site, which decreased the amount of van der Waals interactions.

The C-H and O-H bonds of glycerol are stretched slightly upon adsorption to the Cu(110) as the results shown in Table 3 and adsorption configurations are mostly parallel to the catalyst surface except for the atop adsorption.

3.4 Discussion

For all of the sites on all of the surfaces, Cu(110) long bridge is conclusively the most favorable docking location, with adsorption energies of -0.53 eV (for DFT) and -1.28 eV (for DFT-D3). In comparison, the most stable docking locations of glycerol on Pt(111) had an adsorption energy of -0.46 eV, Rh(111) had an adsorption energy of -0.47 eV, and Pd(111) had -0.38 eV.[135,136]

For every calculation, the DFT-D3 method increased the adsorption energy and decreased the Cu-O distance. However, the DFT-D3 calculations did not change which surfaces have the highest (Cu(110)) and lowest (Cu(111)) adsorption energies, merely the order of docking site stability on each surface. A study conducted on Pt surfaces had very similar results; glycerol bonded strongest to Pt(110) and weakest to Pt(111), with van der Waals corrections only changing the degree of difference between the surfaces.[122] The DFT-D3 calculations did not seem to have a significant effect on the bond distances of the glycerol, but it did decrease the distance between the Copper and central Oxygen of the glycerol, which likely resulted in the increased adsorption energies.

To better understand the effect of van der Waals interaction to the adsorption, we plotted in Figure 6 the charge density differences in the DFT and DFT-D3 results for three of the Cu(110)

docking sites. The adsorptions on the hollow and long bridge site show the most visible electronic distortion when van der Walls interaction was included in the calculations.

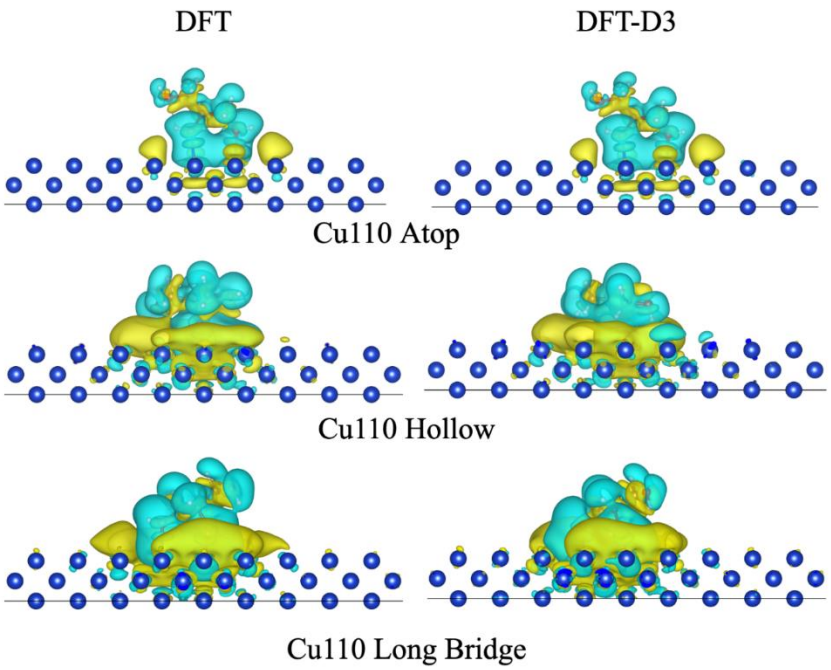

Fig. 6. Charge density difference of glycerol adsorption on Cu(110) using DFT (left) and DFT-D3 (right) with an isosurface cutoff at ±1.5E+-4. Blue is charge deficiency and yellow is charge accumulation.

We point out that different adsorption strengths of glycerol on the three Cu surfaces may also provide selectivity on dehydrogenation of glycerol. Strong adsorptions of ethanol on Ir catalysts indicate that other metals beyond Cu may be a good alloy candidates for better catalytic performance and are worthy of future studies. Activation of C-H or O-H bond is achieved by photons, which follows different mechanism.[26,27,29,137-139] Co-adsorbate, such as water,[140] or hydrogen bond[141] and solvent effect[142] will be interesting in the future studies to consider. Other areas of interest are to understand the effect of alloy on the adsorption of glycerol as previous studies showing promises of alloying effect,[104,107,108,143-147] to modulate the oxidative state of the catalysts,[119,148] or to explore the size of nanocatalysts.[149-152]

4. Conclusions

Calculations using DFT and including the van der Waals interaction correction (DFT-D3) were performed to study the adsorption of glycerol on three Cu surfaces. DFT-D3 results show increased adsorption energies and shorter Cu-O bond lengths than the DFT results. Both calculations predicted that the Cu(110) long bridge site is the most favorable for docking glycerol, but the relative favorability of the other docking sites is different between the two DFT calculations. Charge density difference analysis shows that considerable electrostatic interaction contributes to the increased adsorption under DFT-D3 treatment. The most favorable adsorption configuration is glycerol parallel to the Cu surfaces and majority of the adsorption configurations remains unchanged between the DFT and DFT-D3 results.

Acknowledgements

This research was supported by the NSF REU Program (DMR-2150489) and the Illinois Soybean Center.

References

(1) Almena, A.; Bueno, L.; Dıez, M.; Martın, M. *Clean Techn. Environ. Policy* **2018**, *20*, 1639.
(2) Geraldes, A. N.; Silva, D. F. d.; Silva, L. G. A. e.; Spinacé, E. V.; Neto, A. O. *J. Power Sources* **2015**, *293*, 823.
(3) Neat, S.; Neatu, F.; Chirica, I. M.; Borbath, I.; Talas, E.; Tompos, A.; Somacescu, S.; Osiceanu, P.; Folgado, M. A.; Chaparro, A. M.; Florea, M. *J. Mater. Chem. A* **2021**, *9*, 17065.
(4) Yang, F.; Ye, J.; Yuan, Q.; Yang, X.; Xie, Z.; Zhao, F.; Zhou, Z.; Gu, L.; Wang, X. *Adv. Funct. Mater.* **2020**, *30*, 1908235.
(5) Antolini, E. *Catalysts* **2019**, *9*, 980.
(6) Huang, L.; Yu, X.; Huang, L.; Zhang, X.; Gu, L.; Cao, Y.; Li, W.; Hu, J.; Cao, X. *Green Chem.* **2022**, *24*, 9721.
(7) Ghaith, M. E.; El-Moghny, M. G. A.; El-Nagar, G. A.; Alalawy, H. H.; El-Shakrea, M. E.; El-Deab, M. S. *RSC Adv.* **2023**, *13*, 895.
(8) Panjiara, D.; Pramanik, H. *Ionics* **2020**, *26*, 2435.

(9) Krishnadevi, K.; RatnaKumari, S.; Prasanna, D.; Prasanna, H. B. N.; Anuradha, V. *J. Colloid Interface Sci.* **2022**, *607*, 1776.
(10) Jr., E. F. F.; Barros, V. V. S. d.; Araújo, B. R. S. d.; Purgatto, Â. G.; Linares, J. J. *Int. J. Hydrogen Energy* **2017**, *42*, 23095.
(11) Mello, G. A. B.; Buso-Rogero, C.; Herrero, E.; Feliu, J. M. *J. Chem. Phys.* **2019**, *150*, 041703.
(12) Souza, F. M.; Böhnstedt, P.; Pinheiro, V. S.; Paz, E. C.; Parreira, L. S.; Batista, B. L.; Santos, M. C. *ChemElectroChem* **2019**, *6*, 5396.
(13) Lertthahan, P.; Yongprapat, S.; Therdthianwong, A.; Therdthianwong, S. *Int. J. Hydrogen Energy* **2017**, *42*, 9202.
(14) Chong, R.; Wang, B.; Li, D.; Chang, Z.; Zhang, L. *Solar Energy Mater. Solar Cells* **2017**, *160*, 287.
(15) Liu, B.-C.; Chen, S.-L.; Ling, X.-Y.; Li, Q.-X.; Xu, C.-W.; Liu, Z.-L. *RSC Adv.* **2020**, *10*, 24705.
(16) Tseng, Y. J.; Scott, D. *Energies* **2018**, *11*, 2259.
(17) Olivares-Ramírez, J. M.; Dector, A.; Bañuelos-Días, J. A.; Amaya-Cruz, D. M.; Ortiz-Verdín, A.; Jiménez-Sandoval, O.; Sabaté, N.; Esquivel, J. P. *Fuel Cells* **2019**, *19*, 10.
(18) Fernandez-Caso, K.; Pena-Rodríguez, A.; Solla-Gullon, J.; Montiel, V.; Díaz-Sainz, G.; Alvarez-Guerra, M.; Irabien, A. *J. CO_2 Util.* **2023**, *70*, 102431.
(19) Raman, A. A. A.; Tan, H. W.; Buthiyappan, A. *Front. Chem.* **2019**, *7*, 774.
(20) Estevez, R.; Aguado-Deblas, L.; Luna, D.; Bautista, F. M. *Energies* **2019**, *12*, 2364.
(21) Smirnov, A. A.; Selishcheva, S. A.; Yakovlev, V. A. *Catalysts* **2018**, *8*, 595.
(22) Anitha, M.; Kamarudin, S. K.; Kofli, N. T. *Chem. Eng. J.* **2016**, *295*, 119.
(23) Wang, T.; Weerasinghe, K. C.; Liu, D.; Li, W.; Yan, X.; Zhou, X.; Wang, L. *J. Mater. Chem. C* **2014**, *2*, 5466.
(24) Zhou, X.; Liu, D.; Wang, T.; Hu, X.; Guo, J.; Weerasinghe, K. C.; Wang, L.; Li, W. *J. Photochem. Photobiol. A: Chem.* **2014**, *274*, 57.
(25) Sun, H.; Liu, D.; Wang, T.; Lu, T.; Li, W.; Ren, S.; Hu, W.; Wang, L.; Zhou, X. *ACS Appl. Mater. Interfaces* **2017**, *9*, 9880.
(26) Wang, T.; Zhao, C.; Zhang, L.; Lu, T.; Sun, H.; Bridgmohan, C. N.; Weerasinghe, K. C.; Liu, D.; Hu, W.; Li, W.; Zhou, X.; Wang, L. *J. Phys. Chem. C* **2016**, *120*, 25263.
(27) Wang, T.; Weerasinghe, K. C.; Sun, H.; Hu, X.; Lu, T.; Liu, D.; Hu, W.; Li, W.; Zhou, X.; Wang, L. *J. Phys. Chem. C* **2016**, *120*, 11338.
(28) Xu, F.; Testoff, T. T.; Wang, L.; Zhou, X. *Molecules* **2020**, *25*, 4478.
(29) Wang, T.; Weerasinghe, K. C.; Ubaldo, P. C.; Liu, D.; Li, W.; Zhou, X.; Wang, L. *Chem. Phys. Lett.* **2015**, *618*, 142.
(30) Xu, F.; Gong, K.; Liu, D.; Wang, L.; Li, W.; Zhou, X. *Solar Energy* **2022**, *240*, 157.
(31) Venkatesan, S.; Hsua, T.-H.; Wong, X.-W.; Teng, H.; Lee, Y.-L. *Chem. Eng. J.* **2022**, *446*, 137349.
(32) Pettipas, R. D.; Hoff, A.; Gelfand, B. S.; Welch, G. C. *ACS Appl. Mater. Interfaces* **2022**, *14*, 3103.
(33) Ghadwal, R. S. *Acc. Chem. Res.* **2022**, *55*, 457.
(34) Munoz-Garcia, A. B.; Benesperi, I.; Boschloo, G.; Concepcion, J. J.; Delcamp, J. H.; Gibson, E. A.; Meyer, G. J.; Pavone, M.; Pettersson, H.; Hagfeldt, A.; Freitag, M. *Chem. Soc. Rev.* **2021**, *50*, 12450.
(35) Kokkonen, M.; Talebi, P.; Zhou, J.; Asgari, S.; Soomro, S. A.; Elsehrawy, F.; Halme, J.; Ahmad, S.; Hagfeldt, A.; Hashmi, S. G. *J. Mater. Chem. A* **2021**, *9*, 10527.
(36) Huaulmé, Q.; Mwalukuku, V. M.; Joly, D.; Liotier, J.; Kervella, Y.; Maldivi, P.; Narbey, S.; Oswald, F.; Riquelme, A. J.; Anta, J. A.; Demadrille, R. *Nat. Energy* **2020**, *5*, 468.
(37) Xu, F.; Gong, K.; Fan, W.; Liu, D.; Li, W.; Wang, L.; Zhou, X. *ACS Appl. Energy Mater.* **2022**, *5*, 13780.

(38) Mo, X.; Gao, X.; Gillado, A. V.; Chen, H.-Y.; Chen, Y.; Guo, Z.; Wu, H.-L.; Tse, E. C. M. *ACS Nano* **2022**, *16*, 12202.
(39) Morales, D. M.; Jambrec, D.; Kazakova, M. A.; Braun, M.; Sikdar, N.; Koul, A.; Brix, A. C.; Seisel, S.; Andronescu, C.; Schuhmann, W. *ACS Catal.* **2022**, *12*, 982.
(40) Fan, L.; Ji, Y.; Wang, G.; Chen, J.; Chen, K.; Liu, X.; Wen, Z. *J. Am. Chem. Soc.* **2022**, *144*, 7224.
(41) Wu, J.; Liu, X.; Hao, Y.; Wang, S.; Wang, R.; Du, W.; Cha, S.; Ma, X.-Y.; Yang, X.; Gong, M. *Angew. Chem. Int. Ed.* **2023**, *62*, e202216083.
(42) Wan, H.; Dai, C.; Jin, L.; Luo, S.; Meng, F.; Chen, G.; Duan, Y.; Liu, C.; Xu, Q.; Lu, J.; Xu, Z. J. *ACS Appl. Mater. Interfaces* **2022**, *14*, 14293.
(43) Lacerda, L. C. T.; Pires, M. d. S.; Corrêa, S.; Oliveira, L. C. A.; Ramalho, T. C. *Chem. Phys. Lett.* **2016**, *651*, 161.
(44) Katryniok, B.; Meléndez, R.; Bellière-Baca, V.; Rey, P.; Dumeignil, F.; Fatah, N.; Paul, S. *Front. Chem.* **2019**, *7*, 127.
(45) Han, X.; Sheng, H.; Yu, C.; Walker, T. W.; Huber, G. W.; Qiu, J.; Jin, S. *ACS Catal.* **2020**, *10*, 6741.
(46) Liu, B.; Gao, F. *Catalysts* **2018**, *8*, 44.
(47) Gomes, J. F.; Martins, C. A.; Giz, M. J.; Tremiliosi-Filho, G.; Camara, G. A. *J. Catal.* **2013**, *301*, 154.
(48) Houache, M. S. E.; Hughes, K.; Safari, R.; Botton, G. A.; Baranova, E. A. *ACS Appl. Mater. Interfaces* **2020**, *12*, 15095.
(49) Gutierrez, A.; Kaila, R. K.; Honkela, M. L.; Slioor, R.; Krause, A. O. I. *Catal. Today* **2009**, *147*, 239.
(50) Bagheri, S.; Julkapli, N. M.; Yehye, W. A. *Renew. Sustain. Energy Rev.* **2015**, *41*, 113.
(51) Nda-Umar, U. I.; Ramli, I.; Taufiq-Yap, Y. H.; Muhamad, E. N. *Catalysts* **2019**, *9*, 15.
(52) Garcia, A. C.; Kolb, M. J.; Sanchez, C. v. N. y.; Vos, J.; Birdja, Y. Y.; Kwon, Y.; Tremiliosi-Filho, G.; Koper, M. T. M. *ACS Catal.* **2016**, *6*, 4491.
(53) Feng, S.; Yi, J.; Miura, H.; Nakatani, N.; Hada, M.; Shishido, T. *ACS Catal.* **2020**, *10*, 6071.
(54) Luo, H.; Yukuhiro, V. Y.; Fernández, P. S.; Feng, J.; Thompson, P.; Rao, R. R.; Cai, R.; Favero, S.; Haigh, S. J.; Durrant, J. R.; Stephens, I. E. L.; Titirici, M.-M. *ACS Catal.* **2022**, *12*, 14492.
(55) Zhang, Y.; Zhang, X.; Yang, P.; Gao, M.; Feng, J.; Li, D. *Appl. Catal. B* **2021**, *298*, 120634.
(56) Walgode, P. M.; Faria, R. P. V.; Rodrigues, A. E. *Catal. Rev.* **2021**, *63*, 422.
(57) Wan, W.; Ammal, S. C.; Lin, Z.; You, K.-E.; Heyden, A.; Chen, J. G. *Nat. Commun.* **2018**, *9*, 4612.
(58) Mou, H.; Chang, Q.; Xie, Z.; Hwang, S.; Kattel, S.; Chen, J. G. *Appl. Catal. B* **2022**, *316*, 121648.
(59) Lin, Y.-T.; Yang, J.; Mou, C.-Y. *ACS Sustainable Chem. Eng.* **2021**, *9*, 3571.
(60) Verma, A. M.; Laverdure, L.; Melander, M. M.; Honkala, K. *ACS Catal.* **2022**, *12*, 662.
(61) Yang Xiao, J. G., and Arvind Varma; Zhao, Z.-J.; Xiao, G. *AIChE J.* **2017**, *63*, 705.
(62) Zhou, J.; Hu, J.; Zhang, X.; Li, J.; Jiang, K.; Liu, Y.; Zhao, G.; Wang, X.; Chu, H. *J. Catal.* **2020**, *381*, 434.
(63) Xie, T.; Bodenschatz, C. J.; Getman, R. B. *Reat. Chem. Eng.* **2019**, *4*, 383.
(64) Valter, M.; Busch, M.; Wickman, B. r.; Grönbeck, H.; Baltrusaitis, J.; Hellman, A. *J. Phys. Chem. C* **2018**, *122*, 10489.
(65) Xiao, Y.; Varma, A. *ACS Energy Lett.* **2016**, *1*, 963.
(66) Fernández, P. S.; Gomes, J. F.; Angelucci, C. A.; Tereshchuk, P.; Martins, C. A.; Camara, G. A.; Martins, M. E.; Silva, J. L. F. D.; Tremiliosi-Filho, G. *ACS Catal.* **2015**, *5*, 4227.

(67) Valter, M.; Santos, E. C. d.; Pettersson, L. G. M.; Hellman, A. *J. Phys. Chem. C* **2020**, *124*, 17907.
(68) Santos, E. C. d.; Araujo, R. B.; Valter, M.; Salazar-Alvarez, G.; Johnsson, M.; Bajdich, M.; Abild-Pedersen, F.; Pettersson, L. G. M. *Electrochim. Acta* **2021**, *398*, 139283.
(69) Ahmad, M. S.; Rahim, M. H. A.; Alqahtani, T. M.; Witoon, T.; Lim, J.-W.; Cheng, C. K. *Chemosphere* **2021**, *276*, 130128.
(70) Silva, R. G. D.; Neto, S. A.; Kokoh, K. B.; Andrade, A. R. D. *J. Power Sources* **2017**, *351*, 174.
(71) Zavrazhnov, S. A.; Esipovich, A. L.; Zlobin, S. Y.; Belousov, A. S.; Vorotyntsev, A. V. *Catalysts* **2019**, *9*, 231.
(72) Testa, M. L.; Parola, V. L.; Mesrar, F.; Ouanji, F.; Kacimi, M.; Ziyad, M.; Liotta, L. F. *Catalysts* **2019**, *9*, 148.
(73) Zavrazhnov, S. A.; Esipovich, A. L.; Danova, S. M.; Zlobina, S. Y.; Belousov, A. S. *Kinet. Catal.* **2018**, *59*, 459.
(74) Xie, T.; Sarupria, A.; Getman, R. B. *Mol. Simulation* **2017**, *43*, 370.
(75) Pereira, C. V.; Maia, V. A.; Zambiazi, P. J.; Souza, R. F. B. d.; Antolini, E.; Neto, A. O. *Results Chem.* **2022**, *4*, 100375.
(76) Garcia, A. C.; Birdja, Y. Y.; Tremiliosi-Filho, G.; Koper, M. T. M. *J. Catal.* **2017**, *346*, 117.
(77) Rangarajan, S.; Brydon, R. R. O.; Bhan, A.; Daoutidis, P. *Green Chem.* **2014**, *16*, 813.
(78) Gupta, G.; Roling, L. T. *ChemCatChem* **2023**, *15*, e202201188.
(79) Amaral, R. C.; Tereshchuk, P.; Seminovski, Y.; Silva, J. L. F. D. *J. Phys. Chem. C* **2017**, *121*, 3445.
(80) Shan, N.; Liu, B. *Langmuir* **2019**, *35*, 4791.
(81) Abrahami, S. T.; Chiter, F.; Klein, L. H.; Maurice, V.; Terryn, H.; Costa, D.; Marcus, P. *J. Phys. Chem. C* **2019**, *123*, 22228.
(82) Fontes, E. H.; Ramos, C. E. D.; Ottoni, C. A.; Souza, R. F. B. d.; Antolini, E.; Neto, A. O. *Renew. Energy* **2021**, *167*, 954.
(83) Calaza, F. C.; Baltanás, M. A.; Sterrer, M.; Freund, H.-J. *Topics Catal.* **2019**, *62*, 1053.
(84) Jin, X.; Subramaniam, B.; Chaudhari, R. V.; Thapa, P. S. *AIChE J.* **2016**, *62*, 1162.
(85) Kong, P. S.; Peres, Y.; Daud, W.; Ashri, W. M.; Cognet, P.; Aroua, M. K. *Front. Chem.* **2019**, *7*, 205.
(86) Luo, H.; Barrio, J.; Sunny, N.; Li, A.; Steier, L.; Shah, N.; Stephens, I. E. L.; Titirici, M. M. *Adv. Energy Mater.* **2021**, *11*, 2101180.
(87) Dodekatos, G. S. n., S.; Tüysüz, H. *ACS Catal.* **2018**, *8*, 6301.
(88) Simões, M.; Baranton, S.; Coutanceau, C. *ChemSusChem* **2012**, *5*, 2106−2124.
(89) Houache, M. S. E.; Hughes, K.; Baranova, E. A. *Sustainable Energy Fuels* **2019**, *3*, 1892.
(90) Li, S.; Lai, J.; Luque, R.; Xu, G. *Energy Environ. Sci.* **2016**, *9*, 3097.
(91) Ahmad, M. S.; Ng, K. H.; Chen, C.-L.; Kabir, F.; Witoon, T.; Wu, T. Y.; Cheng, C. K. *Fuel* **2023**, *333*, 126471.
(92) Whitea, J.; Anil, A.; Martín-Yergaa, D.; Salazar-Alvarez, G.; Henriksson, G.; Cornell, A. *Electrochim. Acta* **2022**, *403*, 139714.
(93) Park, M.; Hwang, J.; Jin, S.; Jang, D.; Kim, H. J.; Choi, S. M.; Seo, M. H.; Kim, W. B. *Chem. Eng. J.* **2023**, *466*, 143138.
(94) Amorim, F. M. L.; Crisafulli, R.; Linares, J. J. *Nanomater.* **2022**, *12*, 1315.
(95) Schünemann, S.; Schüth, F.; Tüysüz, H. *Catal. Sci. Technol.* **2017**, *7*, 5614−5624.
(96) Liu, S. S.; Sun, K. Q.; Xu, B. Q. *ACS Catal.* **2014**, *4*, 2226−2230.
(97) Villa, A.; Dimitratos, N.; Chan-Thaw, C. E.; Hammond, C.; Prati, L.; Hutchings, G. J. *Acc. Chem. Res.* **2015**, *48*, 1403−1412.

(98) Yang, P.; Pan, J.; Liu, Y.; Zhang, X.; Feng, J.; Hong, S.; Li, D. *ACS Catal.* **2019**, *9*, 188−199.
(99) Chen, Y.; Salciccioli, M.; Vlachos, D. G. *J. Phys. Chem. C* **2011**, *115*, 18707−18720.
(100) Rahim, S. A. N. M.; Lee, C. S.; Abnisa, F.; Aroua, M. K.; Daud, W. A. W.; Cognet, P.; Pérès, Y. *Sci. Total Environ.* **2020**, *705*, 135137.
(101) Valter, M.; dos Santos, E. C.; Pettersson, L. G. M.; Hellman, A. *J. Phys. Chem. C* **2020**, *124*, 17907−17915.
(102) Lopez-Pedrajas, S.; Estevez, R.; Schnee, J.; Gaigneaux, E. M.; Luna, D.; Bautista, F. M. *Mol. Catal.* **2018**, *455*, 68.
(103) Sobczak, L.; Jagodzinska, K.; Ziolek, M. *Catal. Today* **2010**, *158*, 121.
(104) Baltrusaitis, J.; Valter, M.; Hellman, A. *J. Phys. Chem. C* **2016**, *120*, 1749.
(105) Miao, B.; Wu, Z.-P.; Xu, H.; Zhang, M.; Chen, Y.; Wang, L. *Comput. Mater. Sci.* **2019**, *156*, 175.
(106) Wu, Z.-P.; Miao, B.; Hopkins, E.; Park, K.; Chen, Y.; Jiang, H.; Zhang, M.; Zhong, C.-J.; Wang, L. *J. Phys. Chem. C* **2019**, *123*, 20853.
(107) Miao, B.; Wu, Z.; Zhang, M.; Chen, Y.; Wang, L. *J. Phys. Chem. C* **2018**, *122*, 22448.
(108) Wu, Z.-P.; Shan, S.; Xie, Z.-H.; Kang, N.; Park, K.; Hopkins, E.; Yan, S.; Sharma, A.; Luo, J.; Wang, J.; Petkov, V.; Wang, L.; Zhong, C.-J. *ACS Catal.* **2018**, *8*, 11302.
(109) Lu, J.; Aydin, C.; Browning, N. D.; Wang, L.; Gates, B. C. *Catal. Lett.* **2012**, *142*, 1445.
(110) Miao, B.; Wu, Z.; Xu, H.; Zhang, M.; Chen, Y.; Wang, L. *Chem. Phys. Lett.* **2017**, *688*, 92.
(111) Wu, R.; Wiegand, K. R.; Wang, L. *J. Chem. Phys.* **2021**, *154*, 054705.
(112) Wu, R.; Wang, L. *Chem. Phys. Impact* **2021**, *3*, 100040.
(113) Wu, R.; Wiegand, K. R.; Ge, L.; Wang, L. *J. Phys. Chem. C* **2021**, *125*, 14275.
(114) Wu, R.; Wang, L. *ChemPhysChem* **2022**, *23*, e202200132.
(115) Wu, R.; Wang, L. *J. Phys. Chem. C* **2022**, *126*, 21650.
(116) Colley, S.; Tabatabaei, J.; Waugh, K.; Wood, M. *J. Catal.* **2005**, *236*, 21.
(117) Inui, K.; Kurabayashi, T.; Sato, S.; Ichikawa, N. *J. Mol. Catal. A: Chem.* **2004**, *216* 147.
(118) Wu, R.; Sun, K.; Chen, Y.; Zhang, M.; Wang, L. *Surf. Sci.* **2021**, *703*, 121742.
(119) Xu, H.; Miao, B.; Zhang, M.; Chen, Y.; Wang, L. *Phys. Chem. Chem. Phys.* **2017**, *19*, 26210.
(120) Wu, Z.; Zhang, M.; Jiang, H.; Zhong, C.-J.; Chen, Y.; Wang, L. *Phys. Chem. Chem. Phys.* **2017**, *19*, 15444.
(121) Wu, C.; Wang, L.; Xiao, Z.; Li, G.; Wang, L. *Chem. Phys. Lett.* **2020**, *746*, 137229.
(122) Tereshchuk, P.; S., C. A.; Da Silva, J. L. *J. Phys. Chem. C* **2014**, *118*, 15251.
(123) Wu, R.; Wang, L. *J. Phys. Chem. C* **2020**, *124*, 26953.
(124) Cao, Y.; Ge, Q.; Dyer, D. J.; Wang, L. *J. Phys. Chem. B* **2003**, *107*, 3803.
(125) Wu, C.; Wang, L.; Xiao, Z.; Li, G.; Wang, L. *Phys. Chem. Chem. Phys.* **2020**, *22*, 724.
(126) Wang, L.; Kalyanaraman, C.; McCoy, A. B. *J. Chem. Phys.* **1999**, *110*, 11221.
(127) Billing, G. D.; Wang, L. *J. Phys. Chem.* **1992**, *96*, 2572.
(128) Kresse, G.; Hafner, J. *Phys. Rev. B* **1993**, *47*, 558.
(129) Kresse, G.; Furthmüller, J. *Comput. Mater. Sci.* **1996**, *6*, 15.
(130) Perdew, J. P.; Burke, K.; Ernzerhof, M. *Phys. Rev. Lett.* **1996**, *77*, 3865.
(131) Wang, V.; Xu, N.; Liu, J.-C.; Tang, G.; Geng, W.-T. *Comput. Phys. Commun.* **2021**, *267*, 108033.
(132) Grimme, S.; Antony, J.; Ehrlich, S.; Krieg, H. *J. Chem. Phys.* **2010**, *132*, 154104.
(133) Grimme, S.; Ehlrich, S.; Goerigk, L. *J. Comput. Chem.* **2011**, *32*, 1456.
(134) Tereshchuk, P.; Amaral, R. C.; Seminovski, Y.; Silva, J. L. F. D. *RSC Adv.* **2017**, *7*, 17122.
(135) Liu, B.; Greeley, J. *J. Phys. Chem. C* **2011**, *115*, 19702.
(136) Liu, B.; Greeley, J. *Phys. Chem. Chem. Phys.* **2013**, *15*, 6475.

(137) Walkup, L. L.; Weerasinghe, K. C.; Tao, M.; Zhou, X.; Zhang, M.; Liu, D.; Wang, L. *J. Phys. Chem. C* **2010**, *114*, 19521.
(138) Fan, X.; Lai, K.; Wang, L.; Qiu, H.; Yin, J.; Zhao, P.; Pan, S.; Xua, J.; Wang, C. *J. Mater. Chem. A* **2015**, *3*, 12179.
(139) Fan, X.; Wu, Z.; Wang, L.; Wang, C. *Chem. Mater.* **2017**, *29*, 639.
(140) Chukwu, K. C.; Arnadottir, L. *ACS Catal.* **2022**, *12*, 789.
(141) Sun, K.; Zhang, M.; Wang, L. *Chem. Phys. Lett.* **2013**, *585*, 89.
(142) Wu, R.; Wang, L. *Phys. Chem. Chem. Phys.* **2023**, *25*, 2190.
(143) Wu, R.; Wang, L. *Chem. Phys. Lett.* **2017**, *678*, 196.
(144) Wu, R.; Wang, L. *Comput. Mater. Sci.* **2021**, *196*, 110514.
(145) Wang, L.; Ore, R. M.; Jayamaha, P. K.; Wu, Z.-P.; Zhong, C.-J. *Faraday Discuss.* **2023**, *242*, 429.
(146) Wang, L.; Williams, J. I.; Lin, T.; Zhong, C. J. *Catal. Today* **2011**, *165*, 150.
(147) Sadek, M. M.; Wang, L. *J. Phys. Chem. A* **2006**, *110*, 14306.
(148) Wu, C.; Xiao, Z.; Wang, L.; Li, G.; Zhang, X.; Wang, L. *Catal. Sci. Technol.* **2021**, *11*, 1965.
(149) Zhang, W.; Ran, X.; Zhao, H.; Wang, L. *J. Chem. Phys.* **2004**, *121*, 7717.
(150) Spivey, K.; Williams, J. I.; Wang, L. *Chem. Phys. Lett.* **2006**, *432*, 163.
(151) Yuan, B.; Zhuang, J.; Kirmess, K. M.; Bridgmohan, C. N.; Whalley, A. C.; Wang, L.; Plunkett, K. N. *J. Org. Chem.* **2016**, *81*, 8312.
(152) Bheemireddy, S. R.; Ubaldo, P. C.; Finke, A. D.; Wang, L.; Plunkett, K. N. *J. Mater. Chem. C* **2016**, *4*, 3963.